Title: APEX2 proximity labeling of RNA in bacteria

Authors: Hadi Yassine[1,2], Elizabeta Sirotkin[3], Omer Goldberger[3], Vincent Lawal[1], Daniel B. Kearns[1], Orna Amster-Choder[3], and Jared M. Schrader[1,2]*

[1]Department of Biology, Indiana University, Bloomington, IN, 47405, USA

[2]Departments of Chemistry and Biological Sciences, Wayne State University, Detroit, MI 48202, USA

[3]Department of Microbiology and Molecular Genetics, IMRIC, The Hebrew University Faculty of Medicine, Jerusalem 91120, Israel

*Corresponding Author: jaschrad@iu.edu

Highlights:

- APEX2 proximity labeling can be applied to RNA in bacteria
- APEX2 RNA labeling reactions occur on the sub-minute timescale.
- APEX2 workflow requires less material and time than current methods.
- Alkyne-Phenol APEX2 substrate provides flexibility with click-chemistry.

Motivation:

Studies over the past several years have shown that distinct RNAs can be targeted to subcellular locations in bacterial cells. The ability to investigate localized RNAs in bacteria is currently limited to imaging-based approaches or to laborious procedures to isolate ribonucleoprotein complexes by grad-seq, HITS-CLIP, or Rloc-seq. However, a major challenge in studying mRNA localization in bacterial cells is that bacterial mRNAs typically last for only a few minutes in the cell, while experiments to investigate their localization or interaction partners can take much longer. Therefore, rapid methods of studying RNA localization are needed to bridge this technical challenge.

Summary:

Rapid spatially controlled methods are needed to investigate RNA localization in bacterial cells. APEX2 proximity labeling was shown to be adaptable to rapid RNA labeling in eukaryotic cells, and through the fusion of APEX2 to different proteins targeted to different subcellular locations, has been useful to identify RNA localization in these cells. Therefore, we adapted APEX2 proximity labeling of RNA to bacterial cells by generating an APEX2 fusion to the RNase E gene, which is necessary and sufficient for BR-body formation. APEX2 fusion is minimally perturbative and RNA can be rapidly labeled on the sub-minute timescale with Alkyne-Phenol, outpacing the rapid speed of mRNA decay in

bacteria. Alkyne-Phenol provides flexibility in the overall downstream application with copper catalyzed click-chemistry for downstream applications, such as fluorescent dye-azides or biotin-azides for purification. Altogether, APEX2 proximity labeling of RNA provides a useful method for studying RNA localization in bacteria.

Introduction:

Bacterial mRNAs have been found to localize to distinct subcellular locations. At a global level, many mRNAs have been found to be associated with the nucleoid, membrane, or cell poles[1–4] and it has been hypothesized that mRNA localization can be important for proper gene expression. For example, Flagellin mRNA in *Campylobacter jejuni* localizes to the cell poles which may facilitate cotranslational flagellar assembly[5]. In addition, biomolecular condensates, which are non-membrane bound organelles often assembled through phase separation, have been rapidly expanding in bacterial cells, with multiple involved in RNA metabolism[4,6]. Yet the functional significance of localization of RNAs to biomolecular condensates in bacteria has just started to be explored.

GRAD-seq, HITS-CLIP, and Rloc-seq methods[1,7,8] have been successful at identifying RNAs associated with specific RNPs or localized to certain subcellular locations. However, a major difficulty is that bacterial mRNAs are very short lived, and these methods require labeling or isolation times much longer than a typical mRNAs half-life, leading to the potential for false negatives. Therefore, rapid methods are needed to isolate the associated labile bacterial mRNA before they are degraded.

APEX2 proximity labeling allows for spatially controlled and rapid RNA labeling[9–12], making it a useful method to assay for localized bacterial RNAs. In this manuscript, we show that APEX2 proximity labeling can be adapted to bacterial condensates via fusion of the core BR-body scaffold RNase E to APEX2. RNA can be labeled robustly by APEX2, as many bacteria natively produce heme, including *E. coli*, *B. subtilis*, and *C. crescentus*. With the addition of H_2O_2 and Alkyne-Phenol triggering labeling, allowing copper catalyzed click chemistry of Alkyne-Phenol labeled RNA with a variety of azides such as Cy5-azide. This protocol can be used to rapidly label bacterial RNAs by APEX2 on the sub-minute timescale, and which can be rapidly purified via copper catalyzed click chemistry conjugation of biotin-peg3-azide followed by streptavidin purification. Through the fusion of APEX2 to different localized RNA binding proteins in bacteria, APEX2 proximity labeling has the potential to improve our knowledge of RNA localization in bacteria.

Materials and Methods:

REAGENT or RESOURCE	SOURCE	IDENTIFIER

Antibodies		
DYKDDDDK Tag (D6W5B) Rabbit mAb (Binds to same epitope as Sigma-Aldrich Anti-FLAG M2 antibody) #14793	Cell Signaling Technology	Cat. No.:14793S
Goat anti-Rabbit IgG (H+L) Secondary Antibody, HRP	Invitrogen	Cat. No.: 31460
Bacterial and virus strains		
Caulobacter crescentus NA1000	Lucy Shapiro's Lab	N/A
Js767 (C. crescentus RNE-Apex2FlgC-2 kan^R)	This study	N/A
Js768 (C. crescentus RNE-Apex2Flg-EGFPC-2 kan^R)	This study	N/A
Js87 (C. crescentus RNE-msfGFPC-4 gent^R)	Al-Husini *et al.* Mol Cell 2018[13]	N/A
LS4379 (C. crescentus hfq-m2)	Lucy Shapiro's Lab	N/A
Js801 (RNEΔCTD-Apex2FlgC-2 kan^R)	This study	N/A
B. subtilis DK1042 comIQ12L	Konkol *et al.* J Bact. 2013[14]	N/A
DB2579 (B. subtilis amyE::rny-APEX2 spec^R amp^R)	This study	N/A
Escherichia coli MG1655	Orna Amster-Choder's Lab	N/A
Kti162 (E. coli rne-mCherry)	Strahl *et al.*, PLOS Genetics 2015[15]	N/A
ES413 (E. coli rne-mcherry-Apex2 kan^R)	This study	N/A
Chemicals, peptides, and recombinant proteins		
Alkyne-Phenol	MedChemExpress	Cat. No.: HY-131442

HYDROGEN PEROXIDE SOLN., 50%, ACS RGT.	Sigmaaldrich	Cat. No.: 7722-84-1
Sodium ascorbate	Sigmaaldrich	Cat. No.: 134-03-2
TRIzol	Thermofisher scientific	Cat. No.: 15596018
Chloroform	Thermofisher scientific	Cat. No.: AC423550010
2-PROPANOL, ANHYDROUS	Sigmaaldrich	Cat. No.: 67-63-0
Glycogen, RNA grade	Thermofisher scientific	Cat. No.: RO551
ETHANOL-D6 (D, 99%), ANHYD.	Sigmaaldrich	Cat. No.: 1516-08-1
Sodium Acetate (3 M), pH 5.5, RNase-free	Thermofisher scientific	Cat. No.: AM9740
Biotin-peg3-Azide	Vector Laboratories	CAS Number: CCT-AZ104
Cy5 Azide	Clickchemistrytools	Cat. No.: AZ118-1
BrightStar™-Plus Positively Charged Nylon Membrane, 30 cm x 45 cm	Thermofisher scientific	Cat. No.: AM10102
UltraPure™ SSC, 20X	Thermofisher scientific	Cat. No.: 15557044
SODIUM HYDROXIDE, PELLETS	Sigmaaldrich	Cat. No.: 1310-73-2
EDTA (0.5 M), pH 8.0, RNase-free	Thermofisher scientific	Cat. No.: AM9261

Sodium Dodecyl Sulfate (98.5%)	Sigmaaldrich	Cat. No.: L3771-500G
Bromophenol Blue	sigmaaldrich	Cat. No.: B0126-25G
Glycerol	sigmaaldrich	Cat. No.: 56-81-5
THPTA	Vectorslab	SKU: CCT-1010-100
Copper(II) sulfate pentahydrate	sigmaaldrich	Cat. No.: 7758-99-8
Bovine Serum Albumin	sigmaaldrich	Cat. No.: 9048-46-8
Thermo Scientific™ Pierce™ ECL Western Blotting Substrate	fisher scientific	Cat. No.: PI32109
Heparin sodium salt from porcine intestinal mucosa	sigmaaldrich	Cat. No.: 9041-08-1
Tris (1 M), pH 7.0, RNase-free	Thermofisher scientific	Cat. No.: AM9851
Tris (Tris Base)	GoldBio	Cat. No.: T-400-500
Hydrochloric acid	Carolina	Cat. No.: 867792
SODIUM CHLORIDE, CRYSTAL	Sigmaaldrich	Cat. No.: 7647-14-5
Tween-20	sigmaaldrich	Cat. No.: 9005-64-5
PageRuler™ Plus Prestained Protein Ladder, 10 to 250 kDa	Thermofisher scientific	Cat. No.: 26620
Urea (ACS)	Fisherchemicals	Cat. No.: U15-3

PBS - Phosphate-Buffered Saline (10X) pH 7.4, RNase-free	Thermofisher scientific	Cat. No.: AM9624
Agar	Fisherchemicals	Cat. No.: DF0001-17-0
Bactopeptone	Thermofisher scientific	Cat. No.: 211677
Yeast extract	sigmaaldrich	Cat. No.: 92144-500G-F
UltraPure™ Ethidium Bromide, 10 mg/mL	Thermofisher scientific	Cat. No.: 15585011
Thermo Scientific™ TriTrack DNA Loading Dye (6X)	Thermofisher scientific	Cat. No.: FERR1161
Thermo Scientific™ GeneRuler 1 kb Plus DNA Ladder, ready-to-use	Thermofisher scientific	Cat. No.: FERSM1334
Magnesium sulfate	sigmaaldrich	Cat. No.: M7506-1KG
Calcium chloride (97%)	sigmaaldrich	Cat. No.: 746495-500G
Kanamycin	Thermofisher scientific	Cat. No.: 11815032
Potassium phosphate dibasic anhydrous	Fisherchemicals	Cat. No.: P288-500
Ammonium Chloride (99.5%)	sigmaaldrich	Cat. No.: A9434-1KG
Sodium phosphate dibasic	sigmaaldrich	Cat. No.: S7907-1KG
Glucose (99.5%)	sigmaaldrich	Cat. No.: G8270-1KG

Luria Broth Base	Thermofisher scientific	Cat. No.: 12795084
Iron (II) sulfate heptahydrate	sigmaaldrich	Cat. No.: F8633-250G
FD Kpn1	Thermofisher scientific	Cat. No.: FD0524
FD EcoR1	Thermofisher scientific	Cat. No.: FD0274
FD EcoRV	Thermofisher scientific	Cat. No.: FD0303
FD Dpn1	Thermofisher scientific	Cat. No.: ER1701
Hifi DNA Assembly Master Mix	NEB	Cat. No.: E2621L
T4 DNA Ligase	Thermofisher scientific	Cat. No.: EL0011
Nalidixic Acid	Fisher scientific	Cat. No.: 50488853
Gentamycin Sulfate	sigmaaldrich	Cat. No.: 345814-1GM
Agarose	Alkali	Cat. No.: A7705
RNAprotect Bacteria Reagent	Qiagen	Cat. No.: 76506
Rifampicin	Sigmaaldrich	Cat. No.: 557303-1GM
Pierce™ ECL Western Blotting Substrate	Thermofisher scientific	Cat. No.: 32106
GeneJET Gel Extraction Kit	Thermofisher scientific	Cat. No.: K0692
GeneJET Plasmid Miniprep Kit	Thermofisher scientific	Cat. No.: K0503

GeneJET PCR Purification Kit	Thermofisher scientific	Cat. No.: K0702
Glycine (99%)	sigmaaldrich	Cat. No.: G8898
Methanol (NF), Fisher Chemical™	Fisher scientific	Cat. No.: 67-56-1
PVDF Transfer Membranes, 0.2 µm	Thermofisher scientific	Cat. No.: 88520
DTT	sigmaaldrich	Cat. No.: 3483-12-3
Phenol Solution	sigmaaldrich	Cat. No.: 108-95-2
Glass Beads, acid-washed 106µm (~140 U.S. sieve)	sigmaaldrich	Cat. No.: G4649
Phenol:Chloroform 5:1	sigmaladrich	Cat. No.: P1944
Lithium Chloride Solution	sigmaaldrich	Cat. No.: 7447-41-8
Experimental models: Organisms/strains		
Caulobacter crescentus NA1000	T00841	N/A
Escherichia coli K-12 MG1655	T00007	N/A
Bacillus subtilis DK1042 comIQ12L	T00010[14]	N/A
Oligonucleotides		
HY1F: tgctgatgccgactacaaggatgacgatg	Invitrogen	N/A
HY1R: actttcccatacgcgtaacgttcgaattc	Invitrogen	N/A
HY2F: cgttacgcgtatgggaaagtcttacccaac	Invitrogen	N/A
HY2R: ccttgtagtcggcatcagcaaacccaag	Invitrogen	N/A
HY3F: gtacaagtgagctagctgcagcccgggg	Invitrogen	N/A
HY3R: gcagctgcagcttgtcatcgtcatccttgtagtcggc	Invitrogen	N/A

HY4F: cgatgacaagctgcagctgcctcccctg	Invitrogen	N/A
HY4R: tgcagctagctcacttgtacagctcgtccatgc	Invitrogen	N/A
HY5F: ggtcgatgacgagaattcgaacgttacg	Invitrogen	N/A
HY5R: tcgcgcgtggggtaccatgcatattaattaag	Invitrogen	N/A
HY6F: gcatggtaccccacgcgcgagcgcaaca	Invitrogen	N/A
HY6R: tcgaattctcgtcatcgaccacgaccgacacg	Invitrogen	N/A
CtrA forward: actgatgctgaagtctgaagg	Al-Husini *et al.* Mol Cell. 2020[16]	N/A
CtrA reverse: gattgaggtcgagcaggataag	Al-Husini *et al.* Mol Cell. 2020[16]	N/A
5s forward: ccattccgaactcggttcgttaag	Al-Husini *et al.* Mol Cell. 2020[16]	N/A
5s reverse: tggcggcgacctactct	Al-Husini *et al.* Mol Cell. 2020[16]	N/A
8688: aggaggtcgaccatagcaagaggaggtgaaagtatg	IDT	N/A
8689: ctcctgctagcgccagaaccagcagcggagccagcggattttg catactctacggctcgag	IDT	N/A
8692: aggaggctagcatgggaaagtcttacccaactgtg	IDT	N/A
8693: ctcctgcatgcttacttgtcatcgtcatccttgtag	IDT	N/A
F-rne-mch: aacatcaagttggacatcacc	Sigma-Aldrich	N/A
R-rne: ctcttccagctcagc	Sigma-Aldrich	N/A
Recombinant DNA		
pFlgC-2	Thanbichler *et al.* NAR 2011[17]	N/A
pRNE-YFPC-1	Al-Husini *et al.* Mol Cell 2018[13]	N/A
Apex2FlgC-2	This paper	N/A

RNE-Apex2FlgC-2	This paper	N/A
RNE-Apex2Flg-EGFPC-2	This paper	N/A
RNEΔCTD-Apex2FlgC-2	This paper	N/A
pcDNA5/FRT/TO APEX2-GFP	Addgene	Cat. No.: 129640
pDP647 (amyE::Phypsank-rny-apex2 spec amp)	This paper	N/A
pDR111 (amyE::Physpank spec amp)	Gift from David Rudner	N/A

rne-Apex2-KmR (gctgctgctgactacaaggatgacgacgataagGGAAAGT CTTACCCAACTGTGAGTGCTGATTACCAGGACG CCGTTGAGAAGGCGAAGAAGAAGCTCAGAGGC TTCATCGCTGAGAAGAGATGCGCTCCTCTAATGC TCCGTTTGGCATTCCACTCTGCTGGAACCTTTGA CAAGGGCACGAAGACCGGTGGACCCTTCGGAA CCATCAAGCACCCTGCCGAACTGGCTCACAGC GCTAACAACGGTCTTGACATCGCTGTTAGGCTTT TGGAGCCACTCAAGGCGGAGTTCCCTATTTTGA GCTACGCCGATTTCTACCAGTTGGCTGGCGTTG TTGCCGTTGAGGTCACGGGTGGACCTAAGGTTC CATTCCACCCTGGAAGAGAGGACAAGCCTGAG CCACCACCAGAGGGTCGCTTGCCCGATCCCAC TAAGGGTTCTGACCATTTGAGAGATGTGTTTGGC AAAGCTATGGGGCTTACTGACCAAGATATCGTTG CTCTATCTGGGGGTCACACTATTGGAGCTGCAC ACAAGGAGCGTTCTGGATTTGAGGGTCCCTGGA CCTCTAATCCTCTTATTTTCGACAACTCATACTTC ACGGAGTTGTTGAGTGGTGAGAAGGAAGGTCTC CTTCAGCTACCTTCTGACAAGGCTCTTTTGTCTG ACCCTGTATTCCGCCCTCTCGTTGACAAATATGC AGCGGACGAAGATGCCTTCTTTGCTGATTACGCT GAGGCTCACCAAAAGCTTTCCGAGCTTGGGTTT GCTGATGCCtaaattacacgtcttgagcgattgtgtaggctg gagctgcttcgaagttcctatactttctagagaataggaacttcg gaataggaacttcaagatcccctcacgctgccgcaagcactca gggcgcaagggctgctaaaggaagcggaacacgtagaaagcc agtccgcagaaacggtgctgaccccggatgaatgtcagctact gggctatctggacaagggaaaacgcaagcgcaaagagaaag caggtagcttgcagtgggcttacatggcgatagctagactgggc ggttttatggacagcaagcgaaccggaattgccagctggggcgc cctctggtaaggttgggaagccctgcaaagtaaactggatggctt tcttgccgccaaggatctgatggcgcaggggatcaagatctgat caagagacaggatgaggatcgtttcgcatgattgaacaagatgg attgcacgcaggttctccggccgcttgggtggagaggctattcgg ctatgactgggcacaacagacaatcggctgctctgatgccgcc gtgttccggctgtcagcgcaggggcgcccggttctttttgtcaaga ccgacctgtccggtgccctgaatgaactgcaggacgaggcagc gcggctatcgtggctggccacgacgggcgttccttgcgcagctg tgctcgacgttgtcactgaagcgggaagggactggctgctattgg gcgaagtgccggggcaggatctcctgtcatctcaccttgctcctg	Twist Bioscience	N/A

Software and algorithms		
ImageJ	Imagej	https://imagej.net/software/fiji/downloads
Ibright analysis software	Thermofisher scientific	https://www.thermofisher.com/us/en/home/technical-resources/software-downloads/ibright-western-imager.html

66

67 ***In vivo* RNA proximity labeling**

68 APEX2, Alkyne-Phenol, and H_2O_2 are needed for RNA proximity labeling

69 Gram negative bacteria

70 Gram negative bacteria were grown overnight in liquid media at their optimal growth
71 temperature. Once the cultures reached an optical density (OD) of ~0.3-0.6, 2.5 mM of
72 alkyne-phenol was added and incubated for 30 minutes in a shaker incubator at 200 rpm. A
73 100 mM H_2O_2 solution (994 µL H_2O + 6 µL H_2O_2, 50%) was then freshly prepared. 1 mM of
74 H_2O_2 was then added for 45 seconds as the cultures were still shaking. The labeling
75 experiment was carried out again with specific omissions as controls: no alkyne-phenol
76 added, no H_2O_2 added, no alkyne-phenol and H_2O_2 added, different concentrations of
77 alkyne-phenol added (0.5 mM and 1 mM), and different H_2O_2 exposures (15 seconds, 30
78 seconds, and 60 seconds). 4 mL of cell culture were then quickly transferred into two 2 mL
79 Eppendorf tubes and centrifuged at 14,000 rpm for 10-15 seconds. The supernatant was
80 quickly discarded, and the cell pellets were resuspended in 1 mL of 65°C pre-warmed
81 TRIzol. Because proximity labeling requires the folded APEX2 protein, its denaturation in
82 TRIzol can be used to quench the proximity labeling reactions. RNA extraction followed by
83 ethanol precipitation was then carried out. 55 µL of a 10 mM Tris-HCl pH 7.0 (no EDTA)
84 solution was added to dissolve the air-dried RNA pellets. The samples were vortexed
85 briefly to aid resuspension. 5 µL were taken from the samples and placed in new tubes for
86 Agilent Tapestation analyses and cell lysate RNA sequencing.

87 Gram positive bacteria

88 Gram positive bacteria were grown overnight in liquid media at their optimal growth
89 temperature. Once the cultures reached an optical density (OD) of ~0.3-0.6, the cultures
90 were re-inoculated into fresh media at an OD of ~0.05 supplemented with 1 mM isopropyl
91 β-D-thiogalactopyranoside (IPTG) to induce the expression of RNY-APEX2. Once the
92 cultures reached an OD of ~0.4-0.5, 2.5 mM of alkyne-phenol was added and incubated for
93 30 minutes in a shaker incubator at 200 rpm. A 100 mM H_2O_2 solution was then freshly
94 prepared.1 mM of H_2O_2 was then added for 45 seconds as the cultures were still shaking.
95 An equal amount of cold methanol (pre-stored at -80 $_o$C) was then added to the culture
96 solution. The mixture was then quickly vortexed for 5 seconds and centrifuged at 14,000
97 rpm for 10-15 seconds. The cell pellets were resuspended in LETS buffer (1M Tris-HCl, 1M
98 LiCl, 0.5M EDTA, and 10% SDS; for a 4 mL of gram positive cultures, the cell pellets were
99 dissolved in 550 uL of LETS buffer). Both the LETS buffer and bead:phenol solutions were
100 pre-warmed at 75 $_o$C before being used. The solution was then transferred to a tube
101 containing glass beads + phenol (for a 4 mL of gram positive culture, 320 uL of glass beads
102 + 380 uL of phenol were used). The mixture was vortexed for 3 minutes. Chloroform was
103 then added to the mixture and the solution was vortexed for 30 seconds (for a 4 mL of gram
104 positive culture, 400 uL of chloroform was added to the cells + beads solution). The
105 samples were then centrifuged at 3200 x g for 10 minutes. The top aqueous layer was then
106 transferred to a fresh tube containing a phenol:chloroform solution (for a 4 mL of gram
107 positive culture, 550 uL of phenol:chloroform was used). The phenol:chloroform solution
108 was pre-warmed at 75 $_o$C before being used. The mixture was then vortexed for 3 minutes,
109 and the sample was centrifuged at 3200 x g for 10 minutes. The top aqueous layer was then
110 transferred to a fresh tube and RNA precipitation was carried out. 55 µL of a 10 mM Tris-
111 HCl pH 7.0 (no EDTA) solution was added to dissolve the air-dried RNA pellets. The
112 samples were vortexed briefly to aid resuspension.

113 Copper-catalyzed click chemistry reactions

114 Copper-catalyzed click chemistry reactions were then conducted on the labeled RNA. The
115 reactions have a 300 µL total volume and contained: 50 µL of 100 ng/uL RNA (5 µg) + 175 µL
116 H_2O + 12 µL of 125 mM sodium ascorbate + 3 µL of 10 mM Cy5-Azide + 60 µL of a mix of 2.5
117 mM Cu(II)SO_4/12.5 mM THPTA (tris-hydroxypropyltriazolylmethylamine). The reagents were
118 added in the order they are listed. The click reaction was vortexed for 5 seconds and
119 incubated for 10 minutes at room temperature away from light exposure. Afterward, RNA
120 precipitation was conducted and the RNA pellets were resuspended in 50 µL of 10 mM
121 Tris-HCl pH 7.0 and 0.1 mM EDTA. The samples were then subjected to dot blot filtration
122 on a nylon membrane following the manual's instructions of BIO RAD's Bio-Dot® and Bio-

123 Dot SF Microfiltration Apparatus. A nylon membrane was pre-wetted in a 6X SSC solution
124 for at least 10 minutes. The pre-wetted nylon membrane was then assembled into the dot
125 blot apparatus. Vacuuming was applied to the apparatus and tighter sealing was
126 implemented. The wells were then washed 3 times with 1 mL of an ice-cold mixture of 10
127 mM NaOH/1 mM EDTA. Afterward, the 5 µg RNA samples were directly applied to the wells
128 (no RNA dissolution was performed). The wells were washed 3 times with 1 mL of an ice-
129 cold mixture of 10 mM NaOH/1 mM EDTA. The blotted membrane was washed 3 times for
130 5 minutes with a 30 mL solution containing 2X SSC and 0.1% SDS. Fluorescent blot
131 imaging was then visualized using an ibright imaging system at a fluorescent light exposure
132 of 50 ms under the Cy5 channel.

133 <u>RNase A & DNase I treatments</u>

134 5 µg RNA (50 µL of 100 ng/µL of RNA) collected from a proximity labeling reaction (4 mL of
135 *Js767* cells grown in M2G media with 2.5 mM alkyne phenol, 45 seconds H_2O_2) were
136 subjected to either an RNase A (5 µL of 10 mg/mL RNase A) or DNase I (5 µL of 1 U/µL
137 DNase I) treatment. The treated and mock samples were incubated for 2 hours at 37°C.
138 Following the enzyme or mock treatments, the RNA was precipitated and resuspended in
139 50 µL of 10 mM Tris-HCl pH 7.0 and then subjected to the Copper catalyzed click-
140 chemistry reaction with Cy5-azide. Following the 10-minute click reaction incubation, the
141 RNA was then precipitated and subjected to dot blot filtration as previously described.

142 <u>Streptavidin capture of biotin labeled RNA</u>

143 To enrich the transcriptome of BR-bodies, RNA labeled with alkyne-phenol was subjected
144 to the following click chemistry reaction: 50 µL of RNA (total RNA volume) + 175 µL H2O +
145 12 µL of 125 mM sodium ascorbate + 3 µL of 10 mM Biotin-peg3-azide + 60 µL of a mix of
146 2.5 mM Cu(II)SO_4/12.5 mM THPTA. The reagents were added in order as they are listed. The
147 click reaction was vortexed briefly and incubated for 10 minutes at room temperature away
148 from light exposure. RNA precipitation was then conducted and the air-dried RNA pellets
149 were resuspended in 100 µL B&W buffer (5 mM Tris-HCl, pH 7.5, 1 M NaCl, 0.5 mM EDTA,
150 0.1% v/v tween-20). The RNA samples were then immediately used for biotinylated RNA
151 enrichment.

152 High-capacity magnetic streptavidin beads (Vectorslab) were washed three times with 1
153 mL B&W buffer, twice with 1 mL of a mix of 0.1 M NaOH/0.05 M NaCl, and once with 1 mL
154 0.1 M NaCl at room temperature. The beads were then blocked using a blocking buffer (1
155 mg/mL BSA + 1 mg/ml heparin salt, dissolved in B&W buffer) at room temperature for 2
156 hours. The beads were then washed three times with 1 mL of B&W buffer under gently
157 vortexing. Afterward, the 100 µL RNA solution was added to the beads along with an extra

158 100 µL of B&W buffer. The RNA and beads were allowed to mix at room temperature for
159 one hour. The RNA-loaded beads were washed three times with 1 mL of B&W buffer, twice
160 with 1 mL of a PBS solution containing 4 M urea + 0.1% SDS, and twice with 1 mL of just
161 PBS at room temperature. To elute the enriched RNA, 900 uL of 65°C pre-warmed TRIzol
162 was added to the beads and the samples were incubated at 65°C for 10 minutes.
163 Afterward, 200 µL of chloroform was added and the samples were inverted 6-7 times and
164 then were incubated for 5 minutes at room temperature. The samples were centrifuged at
165 14,000 rpm for 10 minutes at 4°C. The upper aqueous layer was transferred to a new
166 Eppendorf tube and the enriched RNA was precipitated as previously described. The air-
167 dried RNA pellets were resuspended in 10 µL of 10 mM Tris-HCl pH 7.0 and 0.1 mM EDTA. 4
168 µL were then used for Agilent Tapestation analysis. The remaining volume could be utilized
169 for the follow-up RNA-seq experiments.

170 <u>RNA quality assessment</u>

171 *Js767 (RNE-Apex2FlgC-2)* was grown in PYE at 28°C overnight and re-inoculated into 5 mL
172 M2G the next day. Once the cultures reached an OD of 1.2, 2.5 mM of alkyne-phenol was
173 added and incubated for 30 minutes in a shaker incubator at 28°C at 200 rpm. 1 mM of
174 H_2O_2 was added to the culture for 45 seconds. Total RNA was then collected and
175 precipitated from 4 mL of culture as previously described using TRIzol. Afterward, 50 µL of
176 100 ng/µL of alkylated RNA were subjected to the following copper catalyzed click-
177 chemistry reaction: 50 µL of 100 ng/µL RNA (5 µg) + 175 µL H_2O + 12 µL of 125 mM sodium
178 ascorbate + 3 µL of 10 mM Cy5-Azide + 15 µL of 100 mM aminoguanidine hydrochloric acid
179 + 60 µL of a mix of 2.5 mM Cu(II)SO_4/12.5 mM THPTA. The click reaction was incubated for
180 10 minutes at room temperature away from light exposure. The RNA from the click reaction
181 was then precipitated and the air-dried RNA pellet was resuspended in 50 µL of 10 mM
182 Tris-HCl pH 7.0 and 0.1 mM EDTA. 250 ng of RNA from the *Js767* RNA lysate and the click
183 reaction RNA were sent for Agilent Tapestation analysis.

184 **RNA precipitation**

185 RNA precipitation was carried out by adding, in order, 2 µL of 1 mg/mL glycogen, 1/10
186 sample volume of 3 M sodium acetate pH 5.5, and 1 sample volume of isopropanol. The
187 sample mixtures were vigorously vortexed and stored at -80°C overnight. The samples were
188 spun for 1 hour at 14,000 rpm. The supernatant was then decanted and 1 mL of ice-cold
189 80% ethanol was added. The samples were spun for 15 minutes at 14,000 rpm. The
190 ethanol was pipetted out and the samples were then spun for 1 minute at 14,000 rpm. Any
191 remaining ethanol was pipetted out and the pellets were allowed to air-dry until they
192 became translucent. The RNA was then resuspended in the buffer of choice.

193 **Western Blot**

194 The following buffers were initially prepared:

195 1) 10X transfering buffer: 144 grams of glycine and 30.2 grams of Tris-Base were
196 dissolved in 900 mL of ddH2O. The buffer volume was adjusted to 1 L of ddH2O and
197 then filtered utilizing a Nalgene Rapid-flow sterile disposable filter unit.
198 2) 10X TBS: 24 grams of Tris-Base and 88 grams of NaCl were dissolved in 900 mL of
199 ddH2O. The pH of the buffer was adjusted to 7.6 utilizing hydrochloric acid. The
200 buffer volume was adjusted to 1 L of ddH2O and then sterilized utilizing a Nalgene
201 Rapid-flow sterile disposable filter unit.
202 3) 1X TBST: 10X TBS was diluted 10-fold with ddH2O to make 1X TBS. 0.1% Tween-20
203 was then added to the 1X TBS solution to make 1X TBST.

204 *NA1000, LS4379 (hfq-m2), and Js767(RNE-Apex2FlgC-2)* were inoculated in PYE and
205 incubated overnight at 28°C until they reached log phase (OD ~0.3-0.6). 1 mL was taken
206 from each culture, placed in 1.5 mL Eppendorf tubes, and centrifuged for 2 minutes at
207 6,000 rpm. The liquid cultures were discarded, and the cells were resuspended in 4X SDS
208 loading dye. 125 µL of 4X SDS loading dye was added to cultures with an OD~0.5. The
209 samples were boiled at 95 °C for 5 minutes then vortexed vigorously. The vortexed samples
210 were quickly spun down and placed on ice. 5 µL of a pre-stained PageRuler marker and 20
211 µL of lysate from each sample were loaded onto an SDS-PAGE gel. 1X transferring buffer
212 was freshly prepared (20 mL of 10X transfer buffer + 20 mL of methanol in 160 mL ddH2O)
213 while the samples were running on the gel. A PVDF transferring membrane was wetted in
214 methanol and 6 blotting papers were wetted using 1X transferring buffer for at least 10
215 minutes. Once the lysate samples on the SDS-PAGE were properly resolved, the gel was
216 placed on top of 3 pre-wetted blotting papers, and 2 mL of 1X transferring buffer was
217 poured on the gel. The PVDF membrane was briefly plunged into the 1X transferring buffer
218 and then placed on top of the gel. The remaining 3 blotting papers were placed on top of
219 the PVDF membrane. The transferring of the lysates from the SDS-PAGE gel to the PVDF
220 membrane occurred by utilizing the BIO-RAD Trans-Blot Turbo Transfer system (1 amps,
221 2.5 volts, 15 minutes). Once the transfer was completed, the PVDF membrane was placed
222 in a new container containing 5% BSA (blocking solution). The container was nutated for 1
223 hour at room temperature. Afterward, the 5% BSA blocking solution was discarded and the
224 PVDF membrane was washed 5 times with ddH2O for 5 minutes per wash. The primary
225 antibody (DYKDDDDK anti-flag tag) was then diluted (1:10000) into a fresh 5% BSA
226 solution. Once the last ddH2O wash was completed, the primary antibody solution was
227 poured on the PVDF membrane, and the container was nutated at 4°C overnight. The
228 following day, the primary antibody solution was discarded and the PVDF membrane was

229 washed 5 times with TBST for 5 minutes per wash. The secondary antibody (goat anti-rabbit
230 secondary antibody, HRP conjugated) was then diluted (1:10000) into a fresh 5% BSA
231 solution. Once the last TBST wash was completed, the secondary antibody solution was
232 poured on the PVDF membrane, and the container was nutated at room temperature for 1
233 hour avoiding light exposure. The secondary antibody solution was then discarded and the
234 PVDF membrane was washed 5 times with TBST for 5 minutes per wash. Following the final
235 washing procedure, a pierce ECL western blotting substrate solution was prepared (1 mL
236 of reagent 1 + 1 mL of reagent 2 were mixed and vigorously vortexed). The PVDF membrane
237 was placed on Seram wrap and the 2 mL substrate solution was poured on top of the
238 membrane. The substrate was incubated on the PVDF membrane at room temperature for
239 5 minutes avoiding light exposure. The membrane was then placed into an iBright imaging
240 system and the signal was detected under the Chemi-blot filter.

241 **Dilution Plates**

242 *NA1000 & Js767 (RNE-Apex2FlgC-2)* were grown in PYE overnight at 28°C. The overnight
243 cultures were diluted into fresh media and incubated at 28°C until the cells reached an OD
244 of ~0.3-0.6. Cells were then diluted to an OD=0.05 in PYE and 4 10-fold serial dilutions
245 were made. 5 µL were spotted from each dilution onto PYE plates. The plates were
246 incubated at 28°C for two days, and images were taken using an ibright imaging system.

247 **Fluorescent Cell Imaging**

248 *Js87 (RNE-msfGFP) & Js768 (RNE-Apex2FlgC-EGFPC-2)* were grown in PYE + gent (0.5
249 µg/mL) and PYE + Kan, respectively, overnight at 28°C. Cells were then fixed on M2G +
250 1.5% agarose pads placed on microscope slides (3051, Thermofisher scientific). Imaging
251 was performed on an epifluorescence microscope with a 100X objective. Specifically,
252 Nikon elements software was used to control a Nikon Eclipse NI-E equipped with a
253 CoolSNAP MYO-CCD camera and a 100x Oil CFI Plan Fluor (Nikon) objective to capture the
254 images.
255
256 **mRNA half-lives measurement**

257 *NA1000* and *Js767 (RNE-Apex2FlgC-2)* were grown in liquid PYE at 28°C overnight. Cells
258 were then serially re-inoculated into liquid M2G and incubated until overnight log phase
259 (OD ~0.3-0.6) was reached. Log phase cultures were then re-inoculated to an OD = 0.05 in
260 25 mL liquid M2G. Before adding rifampicin, at time point 0, 1 mL of cells were added to 2
261 mL of RNAprotect Bacterial reagent (Qiagen) and vortexed for 5 seconds. 200 µg/mL of
262 Rifampicin was administered to the cultures and 1 mL of cells were extracted and added to
263 2 mL of RNAprotect Bacterial reagent at each of the following time points (followed by 5
264 seconds vortexing): 1, 2, 4, and 8 minutes. Cells were incubated at room temperature in
265 the RNAprotect Bacterial reagent for 5 minutes before being spun at 5000 rpm for 5

266 minutes. The bacterial pellets were resuspended in 1 mL of 65°C pre-heated TRizol
267 (Ambion) and incubated at 65°C for 10 minutes. 200 µL of chloroform was then added and
268 the samples were incubated at room temperature for 5 minutes. Subsequently, the
269 samples were centrifuged at 14,000 rpm for 10 minutes at 4°C. The aqueous layer was
270 removed and placed in a new 1.5 mL Eppendorf tube. The RNA was then precipitated and
271 the pellets were resuspended in 50 µL elution buffer (10 mM Tris-HCl, pH=7.0, 0.1 mM
272 EDTA). PCR tubes were filled with a master mix that contained 0.4 µM of *ctrA* forward
273 primer and 0.4 µM of *ctrA* reverse primer, 1X Luna Universal One-Step Reaction Mix, 1X
274 Luna WarmStart RT Enzyme Mix, and water. 100 ng/µL of RNA template was additionally
275 aliquoted into each of the PCR tubes. The samples were mixed well and quickly spun
276 down. A QuantStudio Real-Time PCR apparatus was utilized to conduct and examine the
277 qRT-PCR experiments. The same qRT-PCR experiment was done using instead the 5S
278 forward and reverse primers. To determine the mRNA-decay rates, we fitted a linear curve
279 to the ln (fraction RNA remaining) at each time point. Using a standard curve, the Ct was
280 converted into the quantity of RNA. Each time point's 5S rRNA amount was divided by the
281 amount of 5S rRNA at time point 0. The number obtained at each time point was then used
282 to normalize the amount of *ctrA* at each time point. The natural log of % RNA remaining
283 found in each sample was divided by the natural log of RNA at time point 0. The slopes of
284 the linear curve fit were then converted into mRNA half-life using the following equation:
285 mRNA half-life=−ln(2)/slope.

286 **RNA-seq**

287 Duplicate biological samples were prepared for RNA-seq of the Full-length RNase E-APEX2
288 fusion (JS767) and the RNase E-NTD-APEX2 (JS801). Lysates from each sample, as well as
289 the eluted RNA from affinity purification were prepared for RNA-seq. RNA-seq was
290 performed by IU-Bloomington CGB genomics service facility using the Illumina Tru-seq
291 stranded HT kit. Raw sequencing reads were deposited to the NCBI GEO database with
292 accession number GSE297938. Data analysis was performed similar to Al-Husini *et al.* Mol
293 Cell 2020[16]. RNA reads were stripped of adapters, and tRNA and rRNA reads were aligned
294 to unique file with duplicate copies deleted using bowtie[18], and reads not aligning to tRNA
295 and rRNA were aligned to the *C. crescentus* transcriptional units[19] using bowtie. Genes
296 with fewer than 50 reads mapping to them were omitted from analysis, and the RPKM
297 values were calculated for each sample. The log2 ratio between the RPKM values in the
298 elution and lysate samples were then calculated on all genes with >=50 reads in both
299 elution and lysate samples. Samples with log2(elution/lysate) measurements in all four
300 biological samples were used for comparison for BR-body proximity labeling enrichment.
301 To calculate which RNA types were enriched in BR-bodies, the distribution of enrichment
302 measurements log2(elution RPKM/lysate RPKM) were subjected to a T-test with unequal

303 variance between the BR-body + (JS767) and BR-body – (JS801) strains and the resulting p-
304 values were reported. Raw read count and processed proximity labeling RNA-seq data can
305 be found in Table S3.

306 **Plasmid Construction**

307 pAPEX2-FlgC-2 *Kan*^{R}

308 The pFlgC-2 vector[17] was PCR amplified using primers HY1F & HY1R. APEX2 was PCR
309 amplified using primers HY2F & HY2R from the addgene template #129640. The amplicons
310 were run on a 1% agarose gel and gel extracted using a GeneJET Gel Extraction Kit. The
311 purified vector was Dpn1 treated then column purified using the GeneJET PCR Purification
312 Kit. The Apex2FlgC-2 *Kan*^{R} plasmid was assembled via Gibson assembly (NEB) and
313 transformed into chemically competent DHbeta10 *E. coli* and plated on LB + Kan (50
314 µg/mL) plates. The resulting KanR colonies were minipreped using the GeneJET Plasmid
315 Miniprep Kit and screened via restriction digestion (EcoR1) and the insert sequence was
316 verified by Sanger sequencing (Genewiz).

317 pRNE-Apex2-FlgC-2 *Kan*^{R}

318 The last 534 RNase E (RNE) base pairs were obtained by digesting pRNE-YFPC-1[17] with
319 Nde1 and Kpn1. APEX2FlgC-2 was digested with Nde1 and Kpn1. The digestion reactions
320 were run on a 1% agarose gel and the RNE fragment and Apex2-FlgC-2 vector were gel
321 extracted using a GeneJET Gel Extraction Kit. The RNE fragment and Apex2FlgC-2 vector
322 were ligated using T4 ligase, transformed into chemically competent DHbeta10 *E. coli*, and
323 selected on LB + Kan plates. The resulting KanR colonies were minipreped using the
324 GeneJET Plasmid Miniprep Kit and screened via restriction digestion (EcoRV) and the insert
325 sequence was verified by Sanger sequencing (Genewiz).

326 pRNE-Apex2FlgC-EGFPC-2 *Kan*^{R}

327 The RNE-Apex2FlgC-2 vector was PCR amplified using primers HY3F & HY3R. The EGFP
328 insert was PCR amplified using primers HY4F & HY4R from the addgene template #129640.
329 The amplicons were run on a 1% agarose gel and gel extracted using a GeneJET Gel
330 Extraction Kit. The purified vector was Dpn1 treated then column purified using the
331 GeneJET PCR Purification Kit. The RNE-Apex2FlgC-EGFPC-2 plasmid was assembled via
332 Gibson assembly (NEB) and transformed into chemically competent DHbeta10 E. coli and
333 selected on LB + Kan plates. The resulting KanR colonies were minipreped using the
334 GeneJET Plasmid Miniprep Kit and screened via restriction digestion (EcoRV) and the insert
335 sequence was verified by Sanger sequencing (Genewiz).

336 *pRNEΔCTD-Apex2FlgC-2 Kan^R*

337 The pApex2-FlgC-2 vector[17] was PCR amplified using primers HY5F & HY5R. RNE-NTD was
338 PCR amplified using primers HY6F & HY6R from NA1000 cells. The amplicons were run on
339 a 1% agarose gel and gel extracted using a GeneJET Gel Extraction Kit. The purified vector
340 was Dpn1 treated then column purified using the GeneJET PCR Purification Kit. The
341 pRNE(NTD)-Apex2FlgC-2 *Kan^R* plasmid was assembled via Gibson assembly (NEB) and
342 transformed into chemically competent DHbeta10 *E. coli* and plated on LB + Kan (50
343 µg/mL) plates. The resulting KanR colonies were minipreped using the GeneJET Plasmid
344 Miniprep Kit and screened via restriction digestion (Kpn1) and the insert sequence was
345 verified by Sanger sequencing (Genewiz).

346 *pDP647 amyE::Phypsank-rny-apex2 spec^R amp^R*

347 To generate the *B. subtilis* inducible Rny-APEX2 construct pDP647, the *rny* gene was
348 amplified from wild type DK1042 DNA with primers 8688/8689 and *apex2* was amplified
349 from plasmid pAPEXC-2 with primers 8692/8693. Next, the *rny* amplicon was digested
350 with SalI and NheI, the *apex2* amplicon was digested with NheI and SphI and the two
351 fragments were simultaneously ligated into the SalI and SphI sites of pDR111 that carries a
352 polylinker downstream of the IPTG-inducible $P_{hyspank}$ promoter, the gene encoding the LacI
353 repressor, and a spectinomycin resistance cassette between the arms of the amyE gene
354 (generous gift of David Rudner, Harvard Medical School).
355

356 **Strain construction**

357 *Js767: NA1000 rne::rne-apex2-flg Kan^R*

358 The RNE-Apex2FlgC2 plasmid was recombined into the *rne* locus in NA1000 via mating and
359 the selection was carried out on PYE + Nal (20 µg/mL) + Kan (25 µg/ mL) plates. The
360 resulting KanR colonies were first grown in PYE + Kan (5 µg/mL) cultures and then screened
361 by PCR.

362 *Js801: NA1000 rne::rneΔCTD-apex2-flg Kan^R*

363 The RNE*ΔCTD*-Apex2FlgC2 plasmid was recombined into the *rne* locus in NA1000 via
364 mating and the selection was carried out on PYE + Nal (20 µg/mL) + Kan (25 µg/ mL) plates.
365 The resulting KanR colonies were first grown in PYE + Kan (5 µg/mL) cultures and then
366 screened by PCR.

367 *Js768: NA1000 rne::rne-apex2-flg-egfp Kan^R*

368 The RNE-Apex2FlgC-EGFPC-2 plasmid was recombined into the *rne* locus in NA1000 via
369 mating and the selection was carried out on PYE + Kan plates. The resulting KanR colonies
370 were first grown in PYE + Kan cultures and then screened by PCR.

371 *DB2579 amyE::rny-APEX2 spec^R amp^R*

372 The pDP647 plasmid was transformed into DK1042[14] cells, and selected on plates
373 containing LB and 100 µg/mL Spectinomycin. The resulting colonies were then screened
374 for the integration by PCR.

375 *ES413: rne::rne-mcherry-flg-Apex2 kan^R*

376 The *in vitro* synthesized sequence rne-Apex2-KmR was PCR amplified using F-rne-mch and
377 R-rne primers and recombined into the *rne* locus in Kti162[15] by lambda red system[20], the
378 selection was carried out on LB + Kan (30 µg/ mL) plates. The *rne-mcherry-flag-Apex2 kan^R*
379 was then moved to MG1655 by P1 transduction[21]. The resulting Kan^R colonies were grown
380 in LB + Kan, screened by PCR and verified by Sanger sequencing (The Center for Genomic
381 Technologies – Huji).

382 # Results:

383 ## RNaseE-APEX2 proximity labeling of RNA requires Alkyne-Phenol, H_20_2, and
384 APEX2

385 APEX2 is an engineered ascorbate peroxidase which can catalyze the creation of a
386 free radical on the oxygen of alkyne-phenol, and this highly reactive species can react with
387 molecules within a 10-20 nm radius[22,23] (Fig 1A). It was shown that APEX2 can label RNA in
388 eukaryotic cells, making this a useful experimental system for identifying localized
389 RNAs[10,12,24,25]. In order to perform RNA proximity labeling in bacteria, we first generated a
390 gene fusion between RNase E and APEX2. RNase E is known to phase-separate into
391 bacterial ribonucleoprotein bodies (BR-bodies), biomolecular condensates containing
392 mRNA and promoting the mRNA decay process[13,16]. To determine whether APEX2 fusions
393 are tolerated in bacteria, we examined the subcellular localization, cell fitness, and mRNA
394 decay activity of RNase E-APEX2 fusions in the bacterium *Caulobacter crescentus* (Fig 1B).
395 We observed that fusing APEX2 to RNase E led to proper expression of RNase E-APEX2 (Fig
396 S1) and did not alter its ability to phase separate into BR-bodies (Fig 1B). In addition, since
397 RNase E's ability to degrade mRNAs is essential for cell growth[16,26], we also examined the
398 cellular fitness of the RNase E-APEX2 fusion and found that both CFUs and colony size
399 were indistinguishable from wild-type (Fig 1B). Finally, we compared the mRNA decay
400 activity of the RNase E-APEX2 fusion and found that it has similar rates of mRNA decay as
401 compared to wild-type (Fig 1B), while 5S rRNA remained stable. Altogether, we could not

402 detect any measurable differences in RNase E function when fused to APEX2. To examine
403 whether the APEX2 fusion can be used to label RNA we added all combinations of
404 proximity labeling reactants (H_2O_2 and Alkyne-Phenol) in combination with or without the
405 RNase E-APEX2 fusion (Fig 1C). Each of the proximity labeling conditions were performed,
406 and then we extracted the RNA and used copper click chemistry to conjugate a Cy5-azide
407 to the RNA. The RNA was then deposited on a positively charged nylon membrane using a
408 dot blot apparatus, and the Cy5 signal was measured in a fluorescent gel imager. We find
409 that only in the presence of APEX2, H_2O_2, and alkyne-phenol do we observe RNA labeling
410 (Fig 1C), suggesting that APEX2 proximity labeling reactions occurred. To determine
411 whether the Cy5 signal was a result of RNA, or contaminating DNA we performed RNase A
412 or DNase I digestions on our samples before spotting them on the dot blot (Fig 1C). Here
413 we see that RNase A treatment leads to a complete loss of Cy5-fluorescence, while DNase
414 I treatment led to no difference in fluorescence signal, suggesting that our Cy5
415 fluorescence is from RNA.

416 Rapid labeling of cellular RNA with Alkyne-Phenol

417 One of the major challenges of studying bacterial mRNA decay is the very short
418 lifetimes of cellular mRNAs. Most bacterial mRNAs in rapidly growing species have half-
419 lives between 1-4 minutes[27,28], making it hard to harvest the RNA before they are degraded.
420 To address this technical limitation, we first optimized the Alkyne-phenol concentration
421 used for labeling cells and found that 2.5 mM Alkyne-Phenol robustly labels cellular RNA
422 (Fig 2). Next, we performed a time-course of H_2O_2 exposure to identify the timescale of
423 RNA labeling, ranging from 15 seconds reaction times to 1 minute reaction times. We
424 found that robust labeling could be achieved in as little as 15 seconds, while labeling
425 increased upon longer proximity labeling reaction times (Fig 2). Importantly, the labeling
426 reaction occurs on the sub-minutes timescale, making this method well-suited to the use
427 in exponentially growing bacterial cells.

428 RNA proximity labeling works across bacteria

429 To increase the applicability of this method, we sought to determine whether APEX2
430 can label RNA in other species of bacteria. As a key requirement of APEX2 activity is heme,
431 we chose to fuse APEX2 to RNA degradosome scaffold proteins in *E. coli* (gram -) and *B.*
432 *subtilis* (gram +) as both organisms have heme biosynthesis pathways encoded in their
433 genomes. In *E. coli*, we fused APEX2 to RNase E, which scaffolds BR-bodies in this
434 species[15,29], localizing into membrane anchored RNP foci[15]. In *B. subtilis*, we fused APEX2
435 to RNase Y, which scaffolds BR-bodies in this species and also localizes into RNP foci on
436 the inner membrane of the cell[29,30]. In both of these species, we observed RNA labeling
437 after 45 seconds of H_2O_2 incubation that required the APEX2 fusion (Fig 3), suggesting that

438 APEX2 proximity labeling of RNA can be used in diverse species of bacteria which encode
439 heme biosynthesis pathways.

440 Copper click-chemistry of Azide-Biotin and streptavidin purification of labeled 441 RNA.

442 APEX2 proximity labeling of RNA is rather flexible due to the diversity of azides
443 commercially available for copper catalyzed click chemistry. To isolate cellular RNA for
444 RNA-sequencing, we altered the azide from azide-Cy5 dye to azide-biotin to allow for
445 streptavidin-mediated RNA purification from the cell (Fig 4A). In this approach, labeled
446 RNA is extracted from cells and conjugated to azide-biotin using copper catalyzed click
447 chemistry, which allows for the subsequent purification of the labeled RNA using
448 streptavidin-resin. While copper can cleave RNA, using a short incubation time for the
449 click reaction minimizes RNA cleavage by copper (Fig S2). After click chemistry, the RNA
450 can be purified under stringent conditions and eluted from the resin under denaturing
451 conditions. When applied to the RNase E-APEX2 fusion presented earlier, we found that
452 the eluted RNA profile indeed matched that of BR-body RNA isolated via density
453 centrifugation (Fig 4B)[16,31]. To compare the specificity of APEX RNA proximity labeling, we
454 prepared eluted RNAs from BR-body + cells (JS767) and BR-Body – cells (RNaseEΔCTD-
455 APEX2, JS801) and prepared them for RNA-seq. As a control for the initial amount of each
456 RNA in the cell, we also performed RNA-seq on the total RNA lysates of each strain. The
457 overall level of proximity labeling was calculated as the log2 enrichment (eluted/lysate) of
458 each RNA measured at >50 reads/sample. Overall, we found that BR-body + samples
459 (JS767) contained higher overall enrichment levels than BR-body – (JS801) (Fig S3A) whose
460 mean enrichment was near 0, with high reproducibility between biological replicates (Fig
461 S3B). Prior density centrifugation of BR-bodies comparing BR-body + and BR-body –
462 strains found they were enriched in mRNAs, small non-coding RNAs, and antisense RNAs
463 while depleted of tRNAs and rRNAs[16]. Our proximity labeled RNA samples showed mRNAs
464 and small non-coding RNAs were both enriched, while antisense appeared to be enriched,
465 however, the p-value was below a 95% confidence interval (p=0.1), while tRNAs and rRNA
466 were not enriched (Fig 4C). Interestingly, while 16S and 23S rRNA were not enriched, 5S
467 rRNA was enriched, in-line with RNase E's known role of 5S rRNA processing[32,33] and the
468 colocalization of BR-bodies adjacent to rRNA loci *in vivo*[34]. Importantly though, while
469 centrifugation-based isolation of BR-bodies required 200 mL of cell culture and 5 days of
470 hands-on work to isolate the BR-body enriched RNAs[31], APEX2 proximity labeling required
471 only 4 mL of cell culture and 3 days of hands-on work, making it higher throughput.

472 ## Discussion:

473 RNP complexes are important regulators of RNA biology, including transcription, RNA
474 processing, transport, translation, and decay[4,35–37]. In addition to RNP complex formation,
475 these complexes have been increasingly found to localize into biomolecular condensate
476 structures, which help to facilitate the spatial organization of the stages in the mRNA life
477 cycle via phase-separation[4,13,16,38–41]. As realizations that RNA localization has become
478 increasingly important in bacteria, methods to identify the population of localized RNAs
479 have been developed, yet these methods have been limited due to the long timescale of
480 the procedures compared to the short mRNA lifetimes in bacteria. APEX2 proximity
481 labeling can rapidly label RNA and can be easily genetically fused to genes whose proteins
482 have known patterns of subcellular localization. APEX2 proximity labeling of RNA requires
483 small amounts of cells, can be completed in a few hours by a single scientist, and yields
484 sufficient RNA for downstream analysis. The reactivity radius of APEX2 is estimated to be
485 10-20nm[42], suggesting it gives high spatial precision. Genetic fusion of APEX2 is easy to
486 generate, APEX2 RNA labeling works across heme-producing bacteria (*C. crescentus*, *B.*
487 *subtilis*, and *E. coli*), and APEX2 is similar in size to a fluorescent protein and has no
488 observable functional impacts when fused to RNase E, so we anticipate that this is unlikely
489 to disrupt target protein function. The flexibility of click chemistry allows the conjugation
490 of a wide array of clickable fluorophores or clickable affinity substrates as biotin or azide-
491 resin. Altogether, APEX2 proximity labeling of RNA will help to accelerate the discovery of
492 localized RNAs in bacteria.

493 ## Author contributions:

494 HY performed RNA labeling experiments. JMS and HY designed the study and wrote the
495 paper. HY generated *C. crescentus* APEX2 fusions strains. DK generated *B. subtilis* APEX2
496 fusions strains. ES, OG, and OAC generated *E. coli* APEX2 fusion strains.

497 ## Acknowledgements:

498 We thank Tamara Hendrickson for equipment, reagents, and hosting the Schrader lab after
499 it was destroyed in a fire. We thank Dr. Anat Nussbaum-Shochat for technical help in the
500 construction of *ES413 E. coli* strain. NIH grants R35GM124733 to JMS and R35GM131783
501 to DBK. WSU Career Chair Award to JMS. IU startup funds to JMS. NIH T32GM142519-03 to
502 HY. Research in the OAC lab was supported by the Israel Science Foundation (ISF) founded
503 by the Israel Academy of Sciences and Humanities (grant no. 1274/19). OAC is an
504 incumbent of the Dr. Jacob Grunbaum Chair in Medical Sciences.

505 Figure legends:

506 **Figure 1. APEX2 proximity labeling of RNA in bacterial cells with minimal perturbation**.
507 A) Schematic of APEX2 labeling of RNA protocol. The APEX2 protein was fused to RNase E,
508 the major protein that scaffolds BR-bodies. Cells are incubated in media containing
509 alkyne-phenol, and labeled was initiated with H_2O_2. After a brief labeling reaction, RNA was
510 extracted from the cells, and Cy5-azide was conjugated to the RNA by copper catalyzed
511 click chemistry. B) APEX2 fusion does not dramatically impact localization or function
512 (growth rate). Left: *In vivo* localization of RNase E-msfGFP vs RNase E APEX2-msfGFP
513 shows that fusion does not impact the formation of BR-bodies. Scale bar is 1µm. Middle:
514 Growth of RNase E-APEX2 fusion is similar to wild type *Caulobacter* cells. Right: mRNA
515 half-life measurements by qRT-PCR show that RNase E-APEX2 degrades mRNAs with a
516 similar half-life to wild-type. Data are from three biological and technical replicates. C)
517 APEX2 labeling requires H_2O_2 and alkyne-phenol to label RNAs. RNA labeling reactions
518 were placed on a nylon membrane to bind to the RNA in a dot blot apparatus and scanned
519 for Cy5 fluorescence in a gel imager. As a control, the RNA samples were incubated for 2
520 hours with DNase I and RNase A. The RNA was then precipitated before being subjected to
521 the azide-Cy5 click chemistry reaction and was re-precipitated before being filtered on the
522 nylon membrane in the dot blot apparatus.

523 **Figure 2. APEX2 proximity labeling of RNA works rapidly.** Optimization of APEX2 labeling
524 of RNA with Alkyne-Phenol. Top: Alkyne-phenol titration reveals that peak labeling occurs
525 with 2.5 mM Alkyne-Phenol. RNA was labeled in the scheme shown in Fig 1A, and the Cy5
526 intensity was measured in a gel imager. Bottom: Time course of APEX2 labeling. RNA was
527 labeled in the scheme shown in Fig 1A, and RNA labeling is apparent in as short as 15
528 seconds of H_2O_2 incubation, while peak labeling efficiency is observed at 45 seconds of
529 H_2O_2 incubation.

530 **Figure 3. APEX2 proximity labeling of RNA works across species.** APEX2 requires heme
531 for activity, so APEX2 fusions were generated in two additional species with heme
532 biosynthesis pathways, *B. subtilis* (gram +) and *E. coli* (gram –). Both species were and
533 subjected to RNA proximity labeling in mid-exponential phase of growth in LB media at
534 37°C, pre-incubated with alkyne-phenol for 30 minutes, and proximity labeling was
535 triggered by a 45 second incubation with H_2O_2. RNA labeling reactions were subjected to
536 azide-Cy5 click chemistry reactions, and 5 µg RNA placed on a nylon membrane to bind to
537 the RNA in a dot blot apparatus and scanned for Cy5 fluorescence in a gel imager.

538 **Figure 4. APEX2 proximity labeled RNA can be isolated by streptavidin purification**. A)
539 Schematic of the conjugation of biotin-azide to clicked alkyne-phenol and the resulting
540 streptavidin purification. B) Streptavidin purification of biotinylated RNAs. Tapestation

541 RNA profiles of the lysates and elution fractions of biotinylated proximity labeled RNAs.
542 The bottom two bands are tRNAs, which are known to be highly depleted in BR-bodies from
543 differential centrifugation-based isolation of BR-bodies[16,31]. C) RNA-seq enrichment
544 analysis of proximity labeled RNA from BR-body + (RNaseE-APEX2, JS767) and BR-body –
545 (RNaseEΔCTD-APEX2, JS801) cells. Log2 ratio of elution/lysate from each sample is
546 plotted for each RNA quantified. Colored horizontal bars indicate the median values for
547 each distribution. T-test with uneven variance was used to compare the distributions of
548 each RNA type, and RNA types with $p<0.05$ are shown.

549 **Figure S1. RNase E-APEX2-FLAG Western Blot**. Protein lysates generated from *NA1000,*
550 *Hfq-FLAG (LS4379)* and *RNase E-APEX2-FLAG (JS767)* were run on an SDS PAGE gel,
551 transferred to PVDF, and probed with an anti-FLAG antibody.

552 **Figure S2. Effects of copper catalyzed click reaction on RNA integrity**. RNA extracted
553 from APEX2 proximity labeling reactions were ran on an Agilent Tapestation from cells
554 harboring RNase E-APEX2 fusion. The APEX2 labeled RNA was also incubated with Copper
555 Sulfate under similar conditions for click chemistry reactions where we observe minimal
556 RNA degradation from the copper.

557 **Figure S3. RNA-seq data**. A) Log2 enrichment (elution/lysate) for all four RNA proximity
558 labeling biological samples. Mean values are shown in the horizontal bars. B) Correlation
559 plots of the RPKM values between individual biological samples. R^2 values are shown
560 between each sample for reference.

561

562 ## References:

563 1. Kannaiah, S., Livny, J., and Amster-Choder, O. (2019). Spatiotemporal Organization of
564 the E. coli Transcriptome: Translation Independence and Engagement in Regulation.
565 Mol. Cell *76*, 574-589.e7. https://doi.org/10.1016/j.molcel.2019.08.013.

566 2. Irastortza-Olaziregi, M., and Amster-Choder, O. (2021). RNA localization in
567 prokaryotes: Where, when, how, and why. Wiley Interdiscip. Rev. RNA *12*, e1615.
568 https://doi.org/10.1002/wrna.1615.

569 3. Campos, M., and Jacobs-Wagner, C. (2013). Cellular organization of the transfer of
570 genetic information. Curr. Opin. Microbiol. *16*, 171–176.
571 https://doi.org/10.1016/j.mib.2013.01.007.

572 4. Nandana, V., and Schrader, J.M. (2021). Roles of liquid–liquid phase separation in
573 bacterial RNA metabolism. Curr. Opin. Microbiol. *61*, 91–98.
574 https://doi.org/10.1016/j.mib.2021.03.005.

575 5. Dugar, G., Svensson, S.L., Bischler, T., Wäldchen, S., Reinhardt, R., Sauer, M., and
576 Sharma, C.M. (2016). The CsrA-FliW network controls polar localization of the dual-
577 function flagellin mRNA in Campylobacter jejuni. Nat. Commun. *7*, 11667.
578 https://doi.org/10.1038/ncomms11667.

579 6. Azaldegui, C.A., Vecchiarelli, A.G., and Biteen, J.S. (2021). The emergence of phase
580 separation as an organizing principle in bacteria. Biophys. J. *120*, 1123–1138.
581 https://doi.org/10.1016/j.bpj.2020.09.023.

582 7. Darnell, R.B. (2010). HITS-CLIP: panoramic views of protein-RNA regulation in living
583 cells. Wiley Interdiscip. Rev. RNA *1*, 266–286. https://doi.org/10.1002/wrna.31.

584 8. Hör, J., Di Giorgio, S., Gerovac, M., Venturini, E., Förstner, K.U., and Vogel, J. (2020).
585 Grad-seq shines light on unrecognized RNA and protein complexes in the model
586 bacterium Escherichia coli. Nucleic Acids Res. *48*, 9301–9319.
587 https://doi.org/10.1093/nar/gkaa676.

588 9. Li, Y., Tian, C., Liu, K., Zhou, Y., Yang, J., and Zou, P. (2020). A Clickable APEX Probe for
589 Proximity-Dependent Proteomic Profiling in Yeast. Cell Chem. Biol. *27*, 858-865.e8.
590 https://doi.org/10.1016/j.chembiol.2020.05.006.

591 10. Padron, A., Iwasaki, S., and Ingolia, N.T. (2019). Proximity RNA Labeling by APEX-Seq
592 Reveals the Organization of Translation Initiation Complexes and Repressive RNA
593 Granules. Mol Cell *75*, 875-887 e5. https://doi.org/10.1016/j.molcel.2019.07.030.

594 11. Fazal, F.M., Han, S., Parker, K.R., Kaewsapsak, P., Xu, J., Boettiger, A.N., Chang, H.Y.,
595 and Ting, A.Y. (2019). Atlas of Subcellular RNA Localization Revealed by APEX-Seq. Cell
596 *178*, 473-490.e26. https://doi.org/10.1016/j.cell.2019.05.027.

597 12. Zhou, Y., Wang, G., Wang, P., Li, Z., Yue, T., Wang, J., and Zou, P. (2019). Expanding
598 APEX2 Substrates for Proximity-Dependent Labeling of Nucleic Acids and Proteins in
599 Living Cells. Angew. Chem. Int. Ed Engl. *58*, 11763–11767.
600 https://doi.org/10.1002/anie.201905949.

601 13. Al-Husini, N., Tomares, D.T., Bitar, O., Childers, W.S., and Schrader, J.M. (2018). α-
602 Proteobacterial RNA Degradosomes Assemble Liquid-Liquid Phase-Separated RNP
603 Bodies. Mol. Cell *71*, 1027-1039.e14. https://doi.org/10.1016/j.molcel.2018.08.003.

604 14. Konkol, M.A., Blair, K.M., and Kearns, D.B. (2013). Plasmid-encoded ComI inhibits
605 competence in the ancestral 3610 strain of Bacillus subtilis. J. Bacteriol. *195*, 4085–
606 4093. https://doi.org/10.1128/JB.00696-13.

607 15. Strahl, H., Turlan, C., Khalid, S., Bond, P.J., Kebalo, J.M., Peyron, P., Poljak, L., Bouvier,
608 M., Hamoen, L., Luisi, B.F., et al. (2015). Membrane recognition and dynamics of the
609 RNA degradosome. PLoS Genet *11*, e1004961.
610 https://doi.org/10.1371/journal.pgen.1004961.

611 16. Al-Husini, N., Tomares, D.T., Pfaffenberger, Z.J., Muthunayake, N.S., Samad, M.A., Zuo,
612 T., Bitar, O., Aretakis, J.R., Bharmal, M.-H.M., Gega, A., et al. (2020). BR-Bodies Provide
613 Selectively Permeable Condensates that Stimulate mRNA Decay and Prevent Release
614 of Decay Intermediates. Mol. Cell *78*, 670-682.e8.
615 https://doi.org/10.1016/j.molcel.2020.04.001.

616 17. Thanbichler, M., Iniesta, A.A., and Shapiro, L. (2007). A comprehensive set of plasmids
617 for vanillate- and xylose-inducible gene expression in Caulobacter crescentus. Nucleic
618 Acids Res. *35*, e137. https://doi.org/10.1093/nar/gkm818.

619 18. Langmead, B., Trapnell, C., Pop, M., and Salzberg, S.L. (2009). Ultrafast and memory-
620 efficient alignment of short DNA sequences to the human genome. Genome Biol. *10*,
621 R25. https://doi.org/10.1186/gb-2009-10-3-r25.

622 19. Bharmal, M.-H., Aretakis, J.R., and Schrader, J.M. (2020). An Improved Caulobacter
623 crescentus Operon Annotation Based on Transcriptome Data. Microbiol. Resour.
624 Announc. *9*. https://doi.org/10.1128/MRA.01025-20.

625 20. Murphy, K.C. (1998). Use of bacteriophage lambda recombination functions to
626 promote gene replacement in Escherichia coli. J. Bacteriol. *180*, 2063–2071.
627 https://doi.org/10.1128/JB.180.8.2063-2071.1998.

628 21. Thomason, L.C., Costantino, N., and Court, D.L. (2007). E. coli genome manipulation
629 by P1 transduction. Curr. Protoc. Mol. Biol. *Chapter 1*, 1.17.1-1.17.8.
630 https://doi.org/10.1002/0471142727.mb0117s79.

631 22. Kalocsay, M. (2019). APEX Peroxidase-Catalyzed Proximity Labeling and Multiplexed
632 Quantitative Proteomics. In Proximity Labeling: Methods and Protocols, M. Sunbul and
633 A. Jäschke, eds. (Springer), pp. 41–55. https://doi.org/10.1007/978-1-4939-9537-0_4.

634 23. Hung, V., Udeshi, N.D., Lam, S.S., Loh, K.H., Cox, K.J., Pedram, K., Carr, S.A., and Ting,
635 A.Y. (2016). Spatially resolved proteomic mapping in living cells with the engineered
636 peroxidase APEX2. Nat. Protoc. *11*, 456–475. https://doi.org/10.1038/nprot.2016.018.

637 24. Padrón, A., and Ingolia, N. (2022). Analyzing the Composition and Organization of
638 Ribonucleoprotein Complexes by APEX-Seq. Methods Mol. Biol. Clifton NJ *2428*, 277–
639 289. https://doi.org/10.1007/978-1-0716-1975-9_17.

640 25. Weissinger, R., Heinold, L., Akram, S., Jansen, R.-P., and Hermesh, O. (2021). RNA
641 Proximity Labeling: A New Detection Tool for RNA–Protein Interactions. Molecules *26*,
642 2270. https://doi.org/10.3390/molecules26082270.

643 26. Christen, B., Abeliuk, E., Collier, J.M., Kalogeraki, V.S., Passarelli, B., Coller, J.A., Fero,
644 M.J., McAdams, H.H., and Shapiro, L. (2011). The essential genome of a bacterium. Mol
645 Syst Biol *7*, 528–528. https://doi.org/10.1038/msb.2011.58.

646 27. Laalami, S., Zig, L., and Putzer, H. (2014). Initiation of mRNA decay in bacteria. Cell Mol
647 Life Sci *71*, 1799–1828. https://doi.org/10.1007/s00018-013-1472-4.

648 28. Jenniches, L., Michaux, C., Popella, L., Reichardt, S., Vogel, J., Westermann, A.J., and
649 Barquist, L. (2024). Improved RNA stability estimation through Bayesian modeling
650 reveals most Salmonella transcripts have subminute half-lives. Proc. Natl. Acad. Sci.
651 U. S. A. *121*, e2308814121. https://doi.org/10.1073/pnas.2308814121.

652 29. Muthunayake, N.S., Tomares, D.T., Childers, W.S., and Schrader, J.M. (2020). Phase-
653 separated bacterial ribonucleoprotein bodies organize mRNA decay. Wiley Interdiscip.
654 Rev. RNA *11*, e1599. https://doi.org/10.1002/wrna.1599.

655 30. Hamouche, L., Billaudeau, C., Rocca, A., Chastanet, A., Ngo, S., Laalami, S., and
656 Putzer, H. (2020). Dynamic Membrane Localization of RNase Y in Bacillus subtilis.
657 mBio *11*, e03337-19. https://doi.org/10.1128/mBio.03337-19.

658 31. Muthunayake, N.S., Al-Husini, N., and Schrader, J.M. (2020). Differential Centrifugation
659 to Enrich Bacterial Ribonucleoprotein Bodies (BR bodies) from Caulobacter
660 crescentus. STAR Protoc. *1*, 100205. https://doi.org/10.1016/j.xpro.2020.100205.

661 32. Nandana, V., Al-Husini, N., Vaishnav, A., Dilrangi, K.H., and Schrader, J.M. (2024).
662 Caulobacter crescentus RNase E condensation contributes to autoregulation and
663 fitness. Mol. Biol. Cell *35*, ar104. https://doi.org/10.1091/mbc.E23-12-0493.

664 33. Mackie, G.A. (2013). RNase E: at the interface of bacterial RNA processing and decay.
665 Nat. Rev. Microbiol. *11*, 45–57. https://doi.org/10.1038/nrmicro2930.

666 34. Bayas, C.A., Wang, J., Lee, M.K., Schrader, J.M., Shapiro, L., and Moerner, W.E. (2018).
667 Spatial organization and dynamics of RNase E and ribosomes in Caulobacter
668 crescentus. Proc Natl Acad Sci U A *115*, E3712–E3721.
669 https://doi.org/10.1073/pnas.1721648115.

670 35. Waters, L.S., and Storz, G. (2009). Regulatory RNAs in bacteria. Cell *136*, 615–628.
671 https://doi.org/10.1016/j.cell.2009.01.043.

672 36. Olejniczak, M., Jiang, X., Basczok, M.M., and Storz, G. (2022). KH domain proteins:
673 Another family of bacterial RNA matchmakers? Mol. Microbiol. *117*, 10–19.
674 https://doi.org/10.1111/mmi.14842.

675 37. Holmqvist, E., and Vogel, J. (2018). RNA-binding proteins in bacteria. Nat. Rev.
676 Microbiol. *16*, 601–615. https://doi.org/10.1038/s41579-018-0049-5.

677 38. Goldberger, O., Szoke, T., Nussbaum-Shochat, A., and Amster-Choder, O. (2022).
678 Heterotypic phase separation of Hfq is linked to its roles as an RNA chaperone. Cell
679 Rep. *41*, 111881. https://doi.org/10.1016/j.celrep.2022.111881.

680 39. Nandana, V., Rathnayaka-Mudiyanselage, I.W., Muthunayake, N.S., Hatami, A.,
681 Mousseau, C.B., Ortiz-Rodríguez, L.A., Vaishnav, J., Collins, M., Gega, A.,
682 Mallikaarachchi, K.S., et al. (2023). The BR-body proteome contains a complex network
683 of protein-protein and protein-RNA interactions. Cell Rep. *42*.
684 https://doi.org/10.1016/j.celrep.2023.113229.

685 40. Hondele, M., Sachdev, R., Heinrich, S., Wang, J., Vallotton, P., Fontoura, B.M.A., and
686 Weis, K. (2019). DEAD-box ATPases are global regulators of phase-separated
687 organelles. Nature *573*, 144–148. https://doi.org/10.1038/s41586-019-1502-y.

688 41. Krypotou, E., Townsend, G.E., Gao, X., Tachiyama, S., Liu, J., Pokorzynski, N.D.,
689 Goodman, A.L., and Groisman, E.A. (2023). Bacteria require phase separation for
690 fitness in the mammalian gut. Science *379*, 1149–1156.
691 https://doi.org/10.1126/science.abn7229.

692 42. Martell, J.D., Deerinck, T.J., Sancak, Y., Poulos, T.L., Mootha, V.K., Sosinsky, G.E.,
693 Ellisman, M.H., and Ting, A.Y. (2012). Engineered ascorbate peroxidase as a genetically
694 encoded reporter for electron microscopy. Nat. Biotechnol. *30*, 1143–1148.
695 https://doi.org/10.1038/nbt.2375.

696

Fig 1

A. Flow Chart of APEX2 Proximity Labeling of RNA

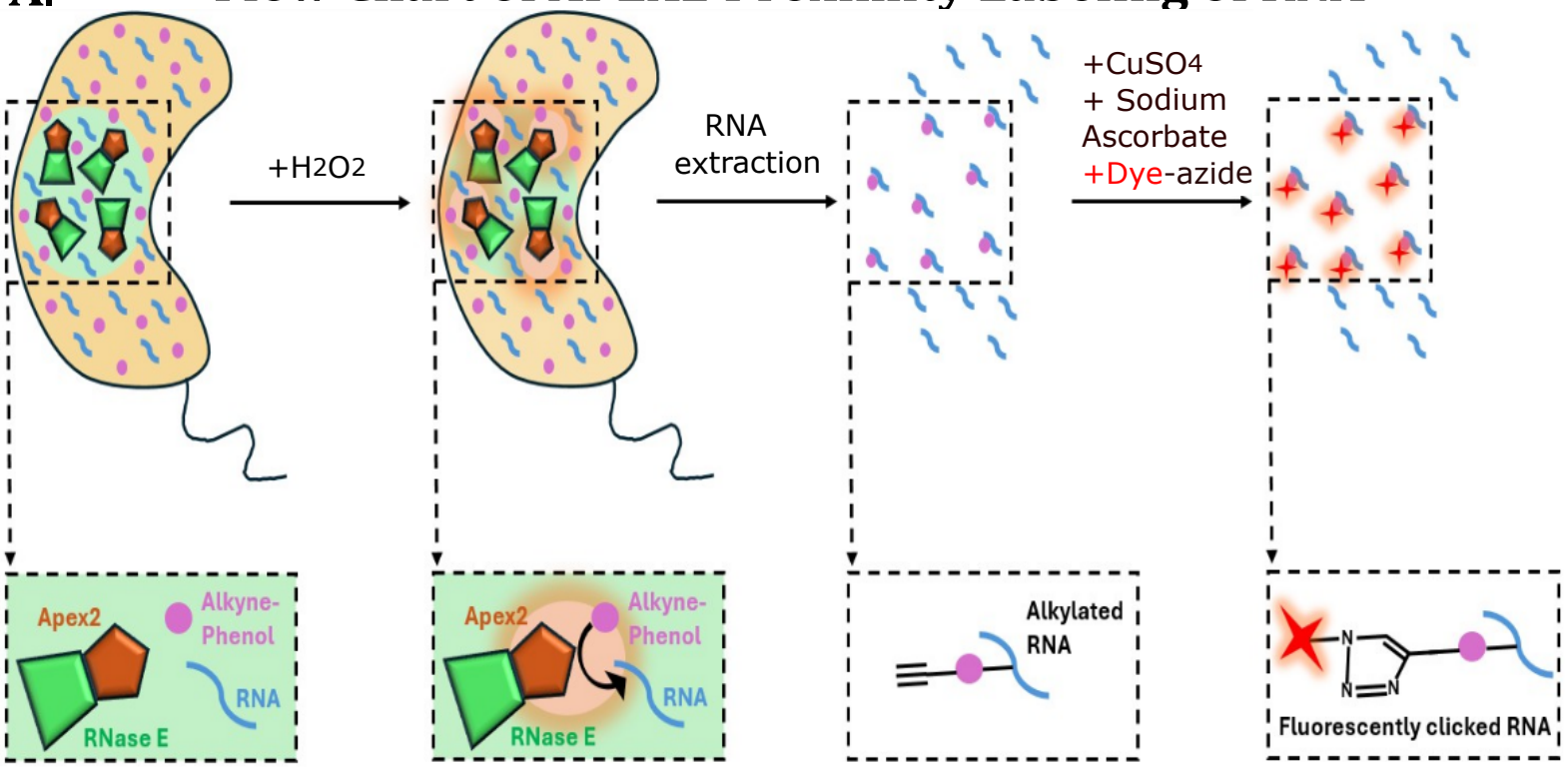

B. APEX2 doesn't impact localization or protein function

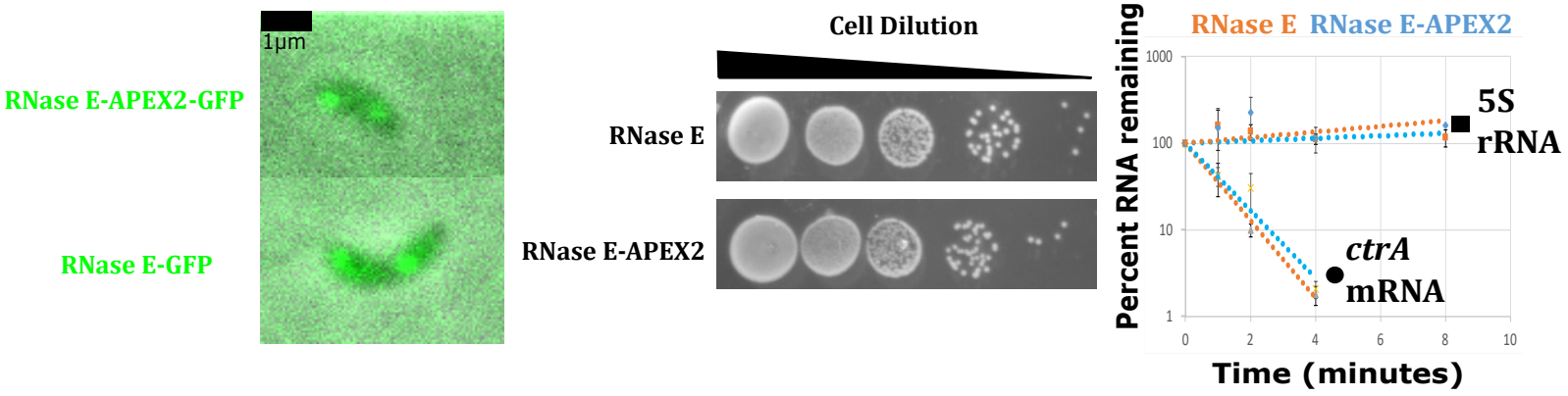

C. APEX2 Proximity Labeling of RNA

APEX2:	−	−	−	−	+	+	+	+
Alk-Ph:	−	+	−	+	−	+	−	+
H_2O_2:	−	−	+	+	−	−	+	+

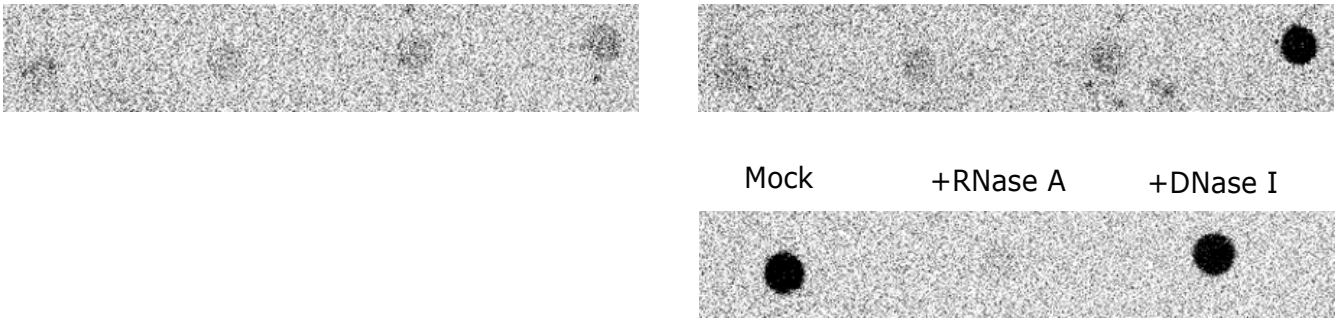

Fig 2

Optimized APEX2 RNA labeling occurs rapidly

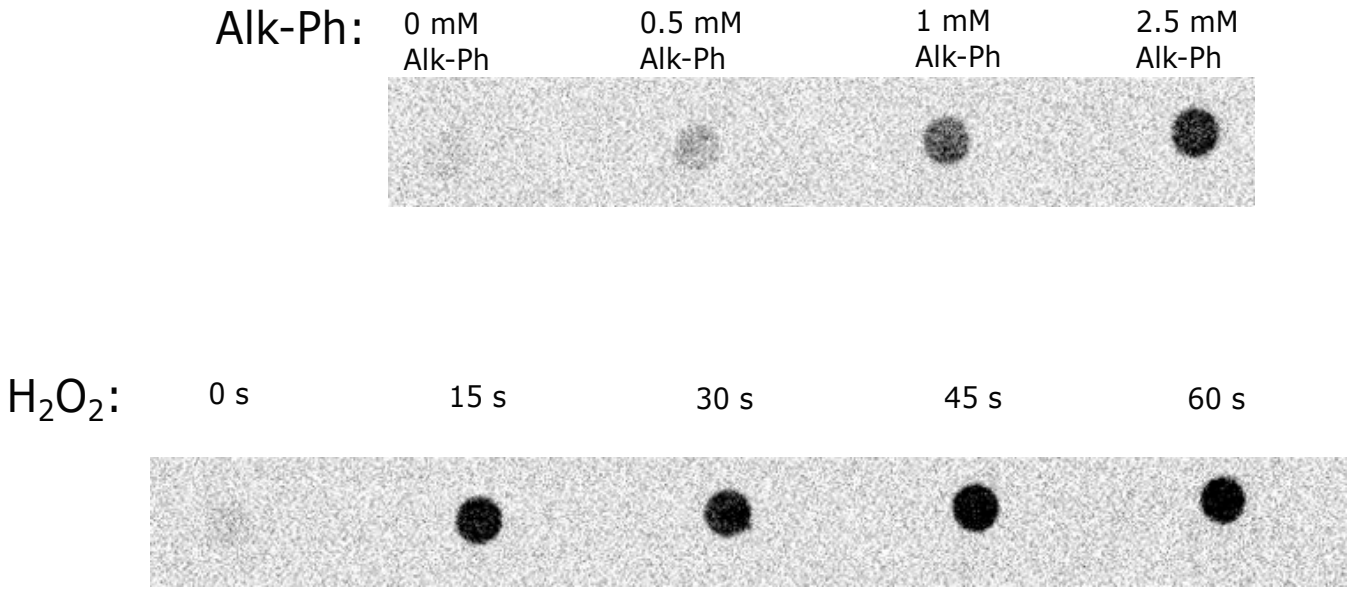

Fig 3

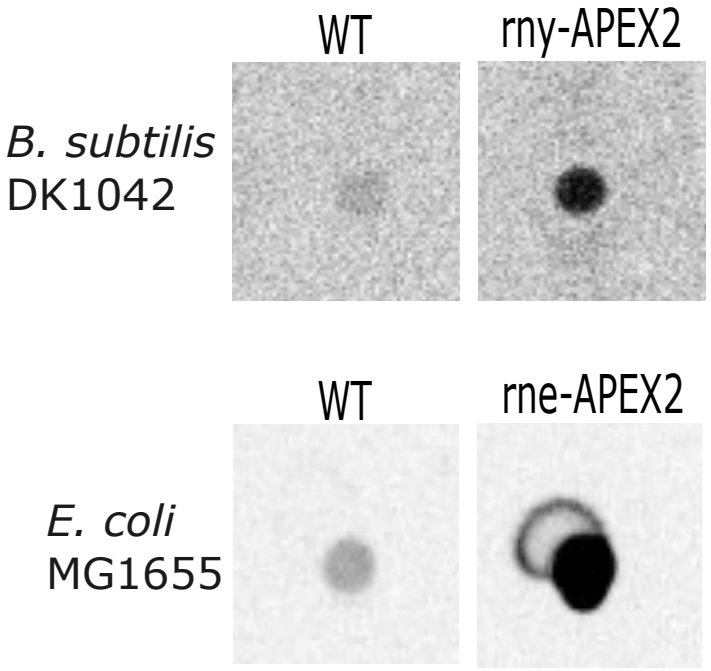

Fig 4

A. APEX2 Proximity Labeling of RNA, clicked with biotin-azide for streptavidin purification

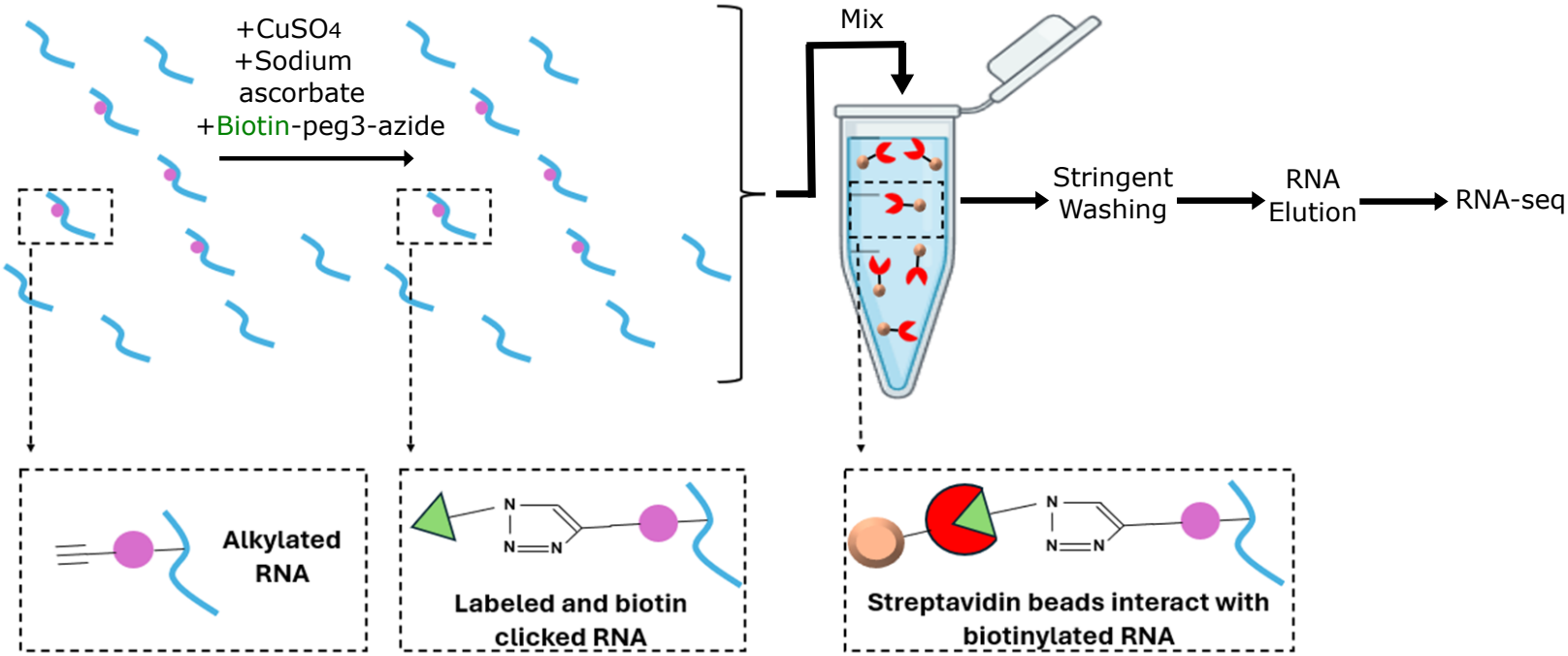

B. Streptavidin purification

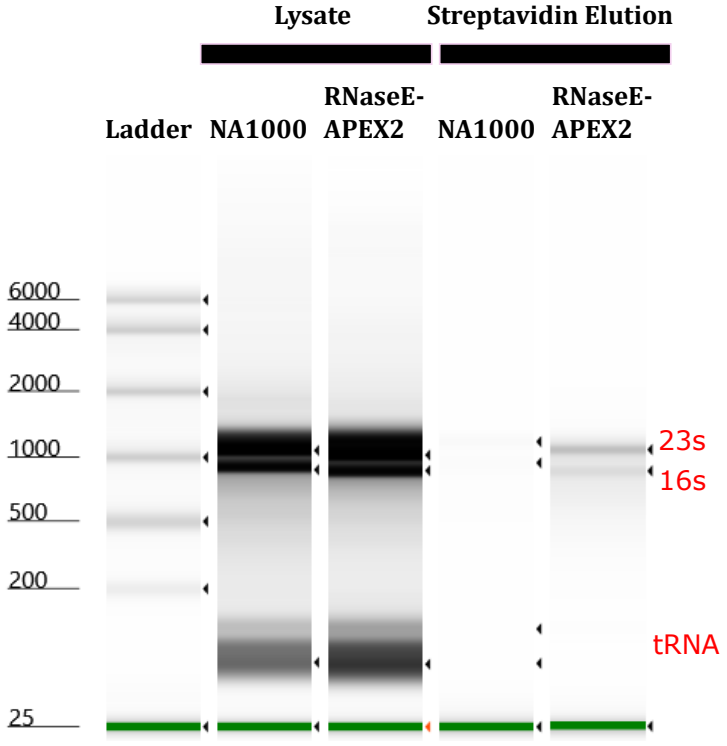
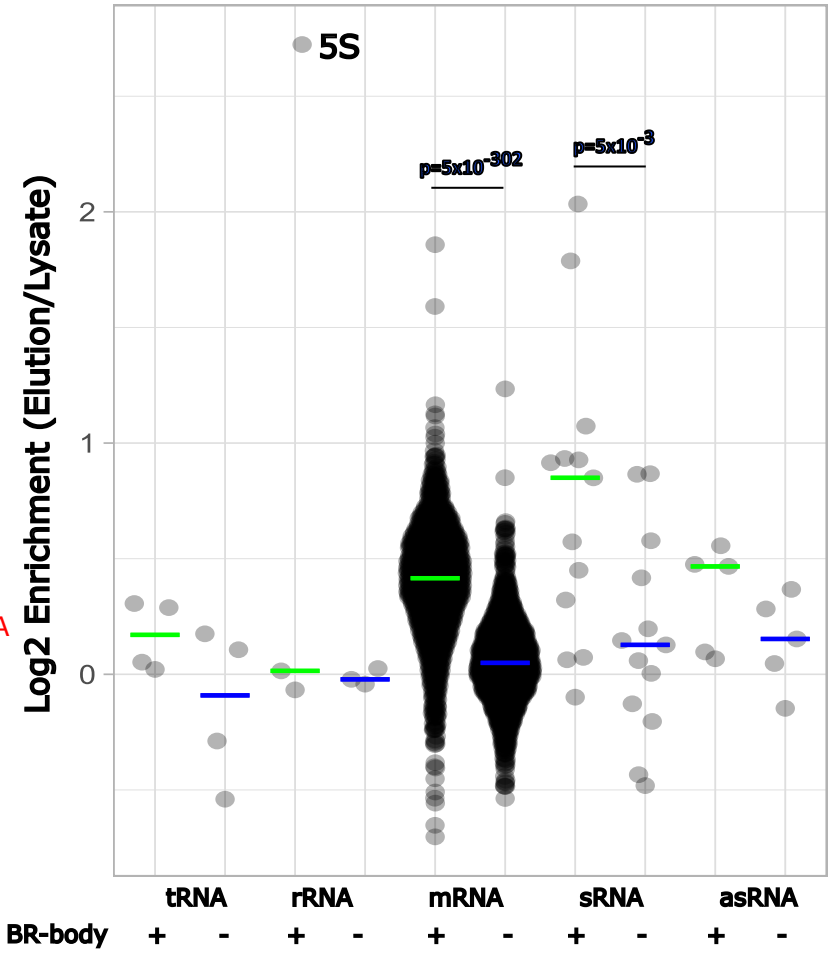
C. RNA-seq enrichment